# 9

*INJURY BIOMECHANICS RESEARCH*
*Proceedings of the Thirty-Fourth International Workshop*

# Investigation of Traumatic Rupture of the Aorta (TRA) using Simulated Real-World Accidents Involving Aortic Injuries

C. S. Shah, W. N. Hardy, K. H. Yang, C. A. Van Ee, R. M. Morgan, and K. H. Digges



## ABSTRACT

*Traumatic rupture of the aorta (TRA) is one of the leading causes of death in automotive crashes. The risk of fatality is higher if the injury is not detected and treated promptly. Numerous laboratory experiments and retrospective studies with focus on TRA have yielded limited success. The use of numerical surrogates has become increasingly important in investigating injuries such as TRA. Four real-world accidents with aortic injuries to the occupants were obtained from the national automotive sampling system (NASS) database. Two crashes were side impact, and two were frontal crashes. Each case was numerically reconstructed in two phases. For the first phase, the car-to-car interaction was simulated using vehicle finite element (FE) models obtained from the national crash analysis center (NCAC) public model archive. They were modified to better represent the actual crash vehicles. These simulations were validated qualitatively and quantitatively against available crash photographs and crush data. For the second phase, the interaction between the occupant and the interior of the automobile was simulated using the results of the first simulation as input. The occupant was a whole-body human FE model developed at Wayne State University (WSU), and represents the mid-sized male. The model includes descriptions of all major thoracic and abdominal organs, major blood vessels including the aorta, and all major bony structures. For the two side impact crashes, the peri-isthmic region demonstrated the greatest maximum principal strain (MPS) and longitudinal stress (LS). For the frontal crashes, the junction of the ascending aorta and the aortic arch was the region of greatest MPS and LS. The strain and stress were computed and compared for the peri-isthmic region of the aorta since it is most relevant to clinically observed TRA. Peak MPS and peak LS averaged within the peri-isthmic region of the aorta for the second phase FE simulations ranged from 0.072 to 0.160, and 0.93 MPa to 1.58 MPa, respectively. The aortic strain and stress patterns and internal kinematics observed in the FE simulations can help to better understand the injury mechanisms of TRA. The results also have application to the design of experiments to study TRA in cadavers.*

## INTRODUCTION

TRA is believed the second most common cause of fatality (Sauaia et al., 1995) associated with motor vehicle crashes (MVC). It is considered to be responsible for approximately 8000 fatalities every year in the United States (Mattox, 1989). Approximately seventy percent of all TRA result from high speed MVC

(Burkhart et al., 2001; Dosios et al., 2000). McGwin et al. (2003) found that TRA occurred predominantly in frontal and near-side impact, corresponding to 45% and 22.5% of the TRA cases, respectively. Even though the overall occurrence of TRA was higher in frontal MVC, the rate of TRA in near-side MVC was found to be twice that in frontal MVC (Steps, 2003). Katyal et al. (1997) found aortic tears confined to the peri-isthmic region of the aorta in ninety-four percent of all TRA. Also, the aortic tears were found nearly always transverse to the long axis of the vessel (Zehnder, 1960). The intima and media of the aorta are typically involved in TRA (Strassmann, 1947; Cammack et al., 1959) and the intact adventitia may temporarily limit the blood loss.

Several theories for TRA injury mechanisms such as downward traction (Letterer, 1924), deceleration (Hass, 1944; Zehnder, 1960; Newman and Rastogi, 1984), intravascular pressure (Oppenheim, 1918; Klotz and Simpson, 1932), osseous pinch (Crass et al., 1990), "Voigt's Shoveling" (Voigt and Wilfert, 1969), and "Water Hammer" (Lundevall, 1964) have been postulated. Various laboratory experiments aimed at producing TRA have yielded limited success. Still, the underlying mechanisms are not very well understood.

Finite element (FE) modeling is becoming an increasingly important tool for understanding the mechanisms of TRA. Shah et al. (2001) developed a FE model of the human thorax. Simulations of thoracic impacts from a number of directions indicated that the ligamentum arteriosum, subclavian artery, parietal pleura, and pressure changes within the aorta are factors that could influence aortic rupture. The aortic isthmus was the most likely site of aortic rupture regardless of impact direction. The human FE thorax model was then integrated with the FE abdomen model (Lee and Yang, 2001) and FE shoulder model (Iwamoto et al. 2000) to develop whole-body human FE model (Shah et al., 2004). Shah et al. (2005a) furthered these modeling efforts by conducting car-to-car simulations and simulating contact of the integrated whole-body human FE model with selected intra-vehicular structures. Similarly, the current study attempts to investigate mechanisms of TRA using simulated real-world MVC involving aortic injuries to the occupants.

## METHODS

Four real-world aortic injury cases were obtained from the NASS database. Several criteria were imposed when selecting these cases. The criteria were gender (male), height (170-180 cm), and weight (68-82 kg) of the subject involved in the crash. Crush deformation (< 70 cm) and Delta-V (< 55 km/hr) were limited to non-catastrophic deformation patterns. For the cases selected, the aorta represented the MAIS injury. Cases of partial or complete ejection and rollover were rejected. The four selected crashes were numerically reconstructed in two phases. Phase 1 consisted of a car-to-car crash simulation. Once the crush characteristics of the case vehicle were acceptably reproduced, a sub-model that included the driver-side structures of the case vehicle was defined and its kinematics saved for the second phase simulation. Phase 2 involved adding the WSU integrated whole-body human FE model of Shah et al. (2004; 2005a) to the sub-model to simulate the interaction of the occupant with the interior of the case vehicle in an effort to correlate model output with potential injury mechanisms and outcomes. For this study, the model was updated to include the pericardium, parietal pleura, and peritoneum. Kinematic joints were also defined for the hip, knee, and ankle joints.

The FE vehicle models were obtained from the NCAC public FE model archive. If the case vehicle or principal other vehicle (POV) were not available in the archive, a model providing the closest dimensional representation was selected and scaled, and the mass adjusted by adding lumped mass at the center of gravity. The occupant masses were adjusted by adding mass to the nodes of the driver and/or passenger seats. The system of units was changed to millimeter, millisecond, and kilogram to make it consistent with the WSU integrated whole-body human FE model. The vehicle sub-models and integrated occupant model were combined in one file for Phase 2 simulations.

For Phase 1 of each simulation, the two vehicles models were initially positioned as suggested by the crash reconstruction data. This required rotation and translation of both vehicle models. The simulation was then setup for the impact. This included construction of a fixed rigid plane to simulate the ground, and definition of contacts between vehicle models as well as contacts between vehicle models and the ground. The heavier of the two vehicles (to maximize energy) is given the appropriate initial velocity. The total simulation time was 150 milliseconds. Structural deformation patterns obtained in the simulations were compared with the real crash data. The simulations were repeated, tuning the impact position of the POV model until a reasonable match was obtained for the case vehicle crush data. For the case vehicles, the driver side structures including the front and rear doorframe, door armrest, and left B-pillar nodes, were grouped and their motions were recorded in separate binary interface files. These interface files were used in the Phase 2 simulations. For frontal simulations, the acceleration pulse obtained at driver's seat during Phase 1 was used for Phase 2 simulation.

For Phase 2 of each simulation, the sub-modeled case vehicle structures interacted with the integrated FE human model. The integrated whole-body human FE model used for this simulation phase was developed at Wayne State University by integrating three component FE models. The integration is detailed by Shah et al. (2004). The model includes a detailed description of the main bony structures, organs, and soft tissues of the human shoulder, thorax and abdomen (Figure 1a). In the trunk region (Figure 1b), the model includes the main organs and vessels. The aorta, vena cava, lungs, heart, spleen, liver, kidneys, pleura, intercostal muscles, shoulder ligaments, shoulder muscles, and their associated tendons are modeled using deformable elements. One airbag representative of the peritoneum was modeled with its visceral reflection covering the liver, spleen, and kidneys. This bag was filled with gas at atmospheric conditions. The organs are surrounded by the rib cage and spine, which are also modeled with deformable elements.

The integrated human FE model was imported into the sub-modeled case vehicle model and was positioned in a seated posture. This posture was estimated based on post-crash photographs of the interior structures and seat. Representative combined vehicle sub-models and the integrated body model for near-side and frontal MVC are shown in Figures 2a and 2b, respectively. Each combined model was then setup for second-phase simulation. A contact interface was created between the vehicle structures and the occupant model. For lateral crashes, the nodal motion of the vehicle structures saved in the interface file was applied to the combined model. For frontal crashes, acceleration pulse was applied to selected vehicle structures.

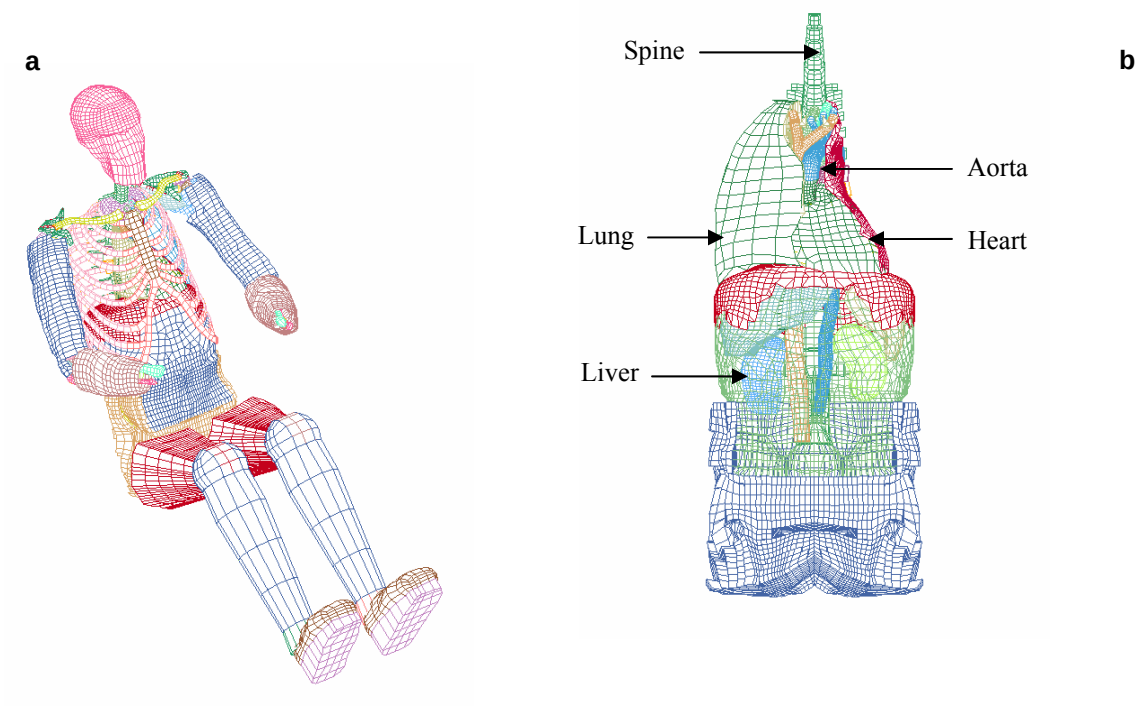


Figure 1: The overall integrated human FE model (a), and the organ details of the same model (b).

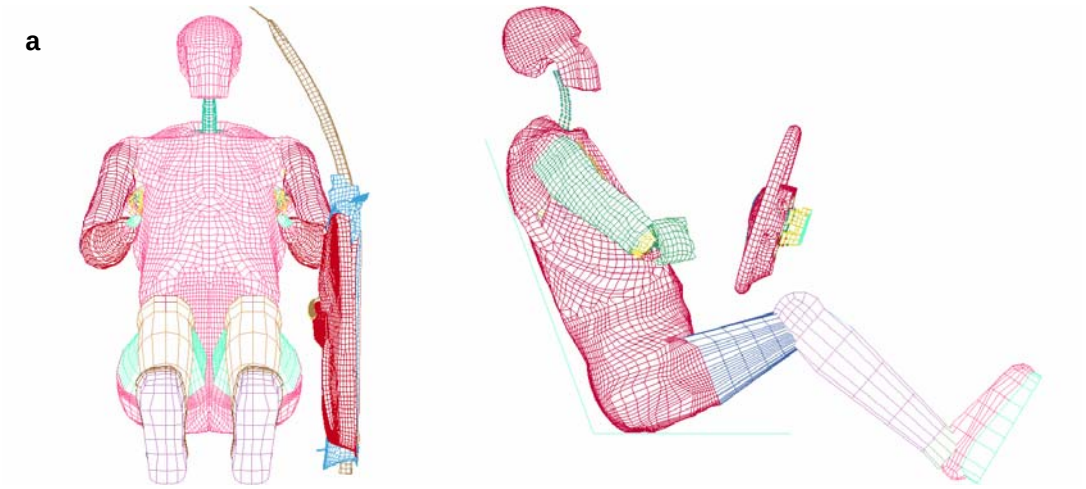


Figure 2: The vehicle substructure and the integrated human FE model positioned for Phase 2 simulation for a typical near side-impact case (a), and a typical frontal-impact case (b).

## Case description

*Case #2000-79-149***.** Vehicle one (V1) was disabled or parked facing southwest in the number-three lane of a five-lane, dry, level, grooved concrete, physically divided roadway. Vehicle two (V2) was north bound in the same lane of the same roadway. The front of V2 impacted the left side of V1 and both cars came to rest in the number-four lane of the same roadway. Both cars were towed from the scene and the driver of V1 (male, 28, 180 cm, 68 kg) was hospitalized for a thoracic aorta laceration (AIS 5) and multiple injuries. The driver of V1 was not wearing any form of belt restraint, but the driver's frontal airbag deployed. Table 1 summarizes the actual crash vehicles and the representations used for the simulation. The mass is the value to which each FE vehicle was adjusted, and the scale factor is the value used to adjust the width and length of the FE vehicles. The Delta-V of the vehicle to which initial speed was applied is also shown. Figure 3a shows the FE setup for the impact simulation.

*Case #1997-11-207***.** V1 was traveling on a two lane rural roadway, approaching an intersection. V2 was traveling east on a two lane rural roadway, approaching the same intersection. The front of V2 contacted the left side of V1 in the intersection. The driver of V1 (male, 58, 155 cm, 68 kg) sustained AIS 4 injury to the thoracic aorta and multiple other injuries, and died. The driver of V1 was wearing a lap belt. The vehicle was not equipped with airbags. The driver of V2 was transported to the emergency room. Both vehicles were towed. Table 1 summarizes the actual crash vehicles and the representations used for the simulation. Figure 3b shows the FE setup for the impact simulation for this case.

*Case #1997-82-214***.** V1 was traveling in the number-1 lane of a 5-lane, two-way street. V2 was traveling in the opposite direction in the number-2 lane of the same road. V1 drifted left and contacted the left front of V2 with its left front. This caused V1 to rotate anticlockwise, and it contacted the front of a third vehicle in the number-3 lane with its right side. The driver of V1 was killed, and a front passenger of V1 sustained minor injuries, as did the driver of V2. The driver of V1 (male, 43, 175 cm, 71 kg) sustained 3 rib fractures and an incomplete laceration (AIS 4) of the thoracic aorta. The driver of V1 was not wearing a seatbelt, and the vehicle was not equipped with airbags. Table 1 summarizes the actual crash vehicles and the representations used for the simulation. Figure 3c shows the FE setup for the impact simulation for this case.

*Case #1998-72-98***.** V1 was traveling north on a two-lane road headed toward a "T" intersection. After stopping, V1 turned left (west) onto the intersecting two-lane road. V2 was headed toward V1 (east) on the intersecting road. The front of V1 hit V2 in the eastbound lane. The driver of V1 (male, 37, 175 cm, 73 kg) sustained a major laceration of the thoracic aorta (AIS 5) and was taken to the hospital. The driver and passenger of V2 were transported to the hospital as well. The driver of V1 was not wearing a seatbelt, and the vehicle was not equipped with airbags. Table 1 summarizes the actual crash vehicles and the representations used for the simulation. Figure 3d shows the FE setup for the impact simulation for this case.

Table 1. Summary of Actual and Simulated Vehicles.

| Case | Vehicle | | Make and Model | Mass (kg) | Scale Factor | Delta-V (km/hr) Total, Longitudinal, Lateral |
|---|---|---|---|---|---|---|
| 2000-79-149 | 1 | actual | 1996 Toyota Corolla | 1052 | | |
| | | simulated | Ford Taurus side impact | | 0.894 | |
| | 2 | actual | 1994 Ford Crown Victoria | 1718 | | |
| | | simulated | Dodge Neon | | 1.150 | 54, -41, 35 |
| 1997-11-207 | 1 | actual | 1992 Saturn SL | 1057 | | |
| | | simulated | Ford Taurus side impact | | 0.943 | |
| | 2 | actual | 1996 Plymouth Breeze | 1331 | | |
| | | simulated | Dodge Neon | | 1.060 | 43, -8, 42 |
| 1997-82-214 | 1 | actual | 1991 Toyota Cressida | 1560 | | |
| | | simulated | Honda Accord frontal impact | | 0.970 | 38, 38, 0 |
| | 2 | actual | 1995 Volvo 850 | 1516 | | |
| | | simulated | Dodge Neon | | 1.000 | |
| 1998-72-98 | 1 | actual | 1989 GMC Sonoma | 1371 | | |
| | | simulated | Chevrolet S10 frontal impact | | 1.000 | |
| | 2 | actual | 1985 Chevrolet Astrovan | 1767 | | |
| | | simulated | Chevrolet C2500 frontal impact | | 1.200 | 46, 46, 0 |

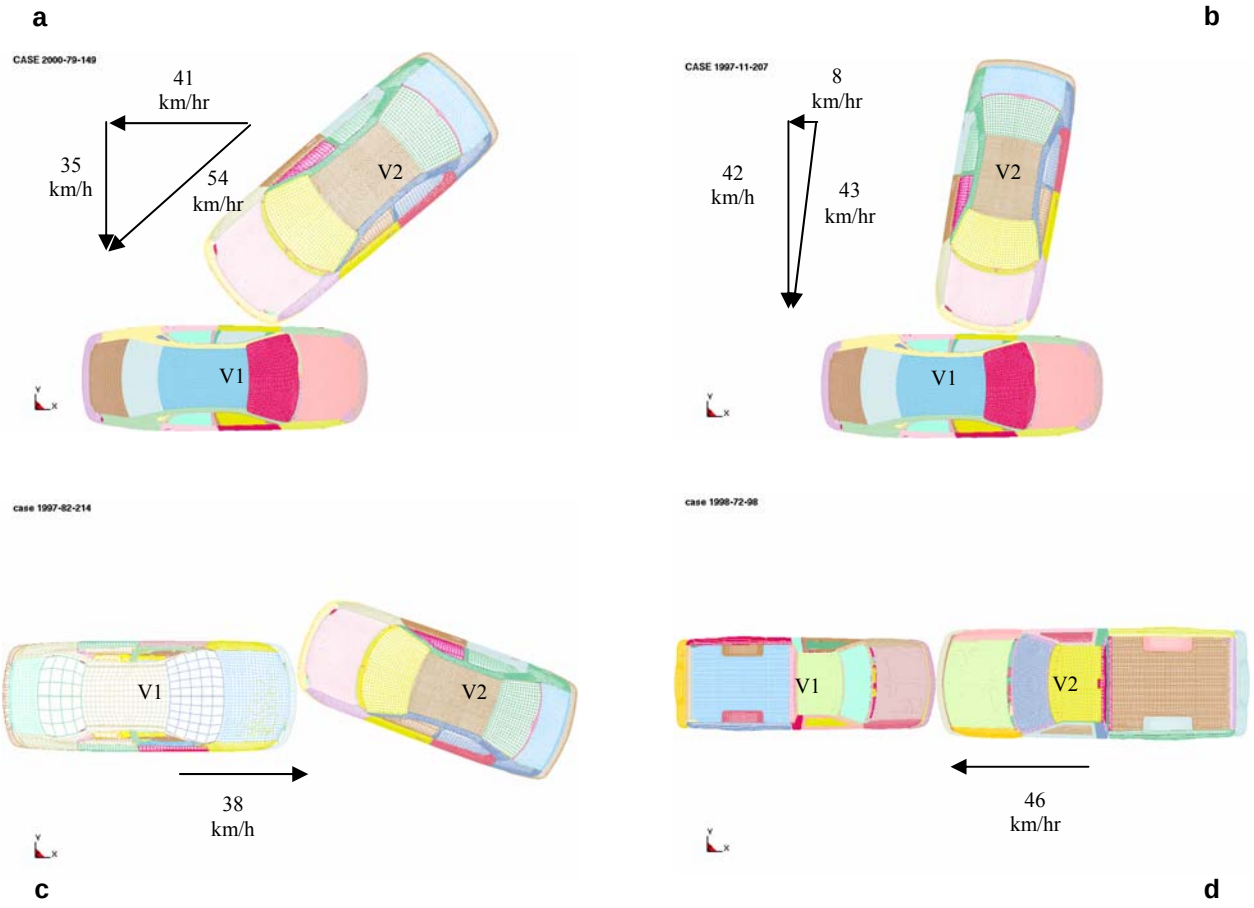


Figure 3: The FE impact setup for case #2000-79-149 (a), case #1997-11-207 (b), case #1997-82-214 (c), and case #1998-72-98 (d).

## RESULTS

Figure 4 shows the deformation patterns of the four case vehicles. Table 2 compares the measured crush values against those achieved during the first phase of FE simulation. The average difference between the actual vehicle deformations and the FE simulations ranged from -2 to -15 percent. Figure 5 shows the occupant interaction with the sub-modeled vehicle components at the time of maximal contact for all four simulations. Time zero is specified as the initial contact between the vehicles. Figure 6 shows the resulting aorta deformation and inner surface maximum principal strain pattern for each of the FE simulations in anterior-posterior (AP) and lateral perspectives for the time of peak strain. The inner surface was examined because tears generally initiate on the inner surface, with the intima tearing first. Table 3 catalogs the average peak aorta response parameters that correspond to the patterns shown in Figure 6. The average peak longitudinal and circumferential true stress, peak Von-mises stress, maximum principal strain, and longitudinal and circumferential Lagrange strains are given as an average from four-to-six elements. The regions selected experienced the largest maximum principal strain within the peri-isthmic region, not associated with the insertion of the ligamentum arteriosum. These values are limited to the peri-isthmic region because in the field it is seen to be preferentially injured, and it is known to be mechanically weaker compared to other regions (Lundevall, 1964). Figure 7 provides the time histories for maximum principal strain, and longitudinal and circumferential Lagrange strain for all four FE cases of aortic injury. The relative time alignment between tests in this figure is arbitrary, and the curves extend to the point beyond which the simulations would not execute. The average longitudinal strains from the side impact simulations are considerably greater than the circumferential strains, and follow the time-history trends of the average maximum principal strains. The average circumferential strain from the frontal impact simulations are greater than the longitudinal strains, and follow the time-history trends of the average maximum principal strains.

Table 2. Comparison Between Actual and Finite Element Crush Values in mm.

| Case # | 2000-79-149 | | 1997-11-207 | | 1997-82-214 | | 1998-72-98 | |
|---|---|---|---|---|---|---|---|---|
| **Point** | **Actual** | **FE** | **Actual** | **FE** | **Actual** | **FE** | **Actual** | **FE** |
| C1 | 0 | * | 160 | * | 650 | 571 | 690 | 580 |
| C2 | 400 | 334 | 700† | 380 | 670 | 546 | 590 | 520 |
| C3 | 600 | 525 | 370 | 448 | 520 | 448 | 630 | 553 |
| C4 | 300 | 265 | 450 | 382 | 310 | 352 | 660 | 574 |
| C5 | 60 | * | 140 | * | 110 | 131 | 530 | 485 |
| C6 | 0 | * | 0 | * | 0 | 0 | 580 | 493 |
| Avg. Δ (%) | | -9.7 | | -3.0 | | -2.4 | | -15.3 |

* Only C2-C4 (door deformation) were compared for the side impact cases.
† The rear door was removed for this measurement, making it artificially large (not used for Δ %).

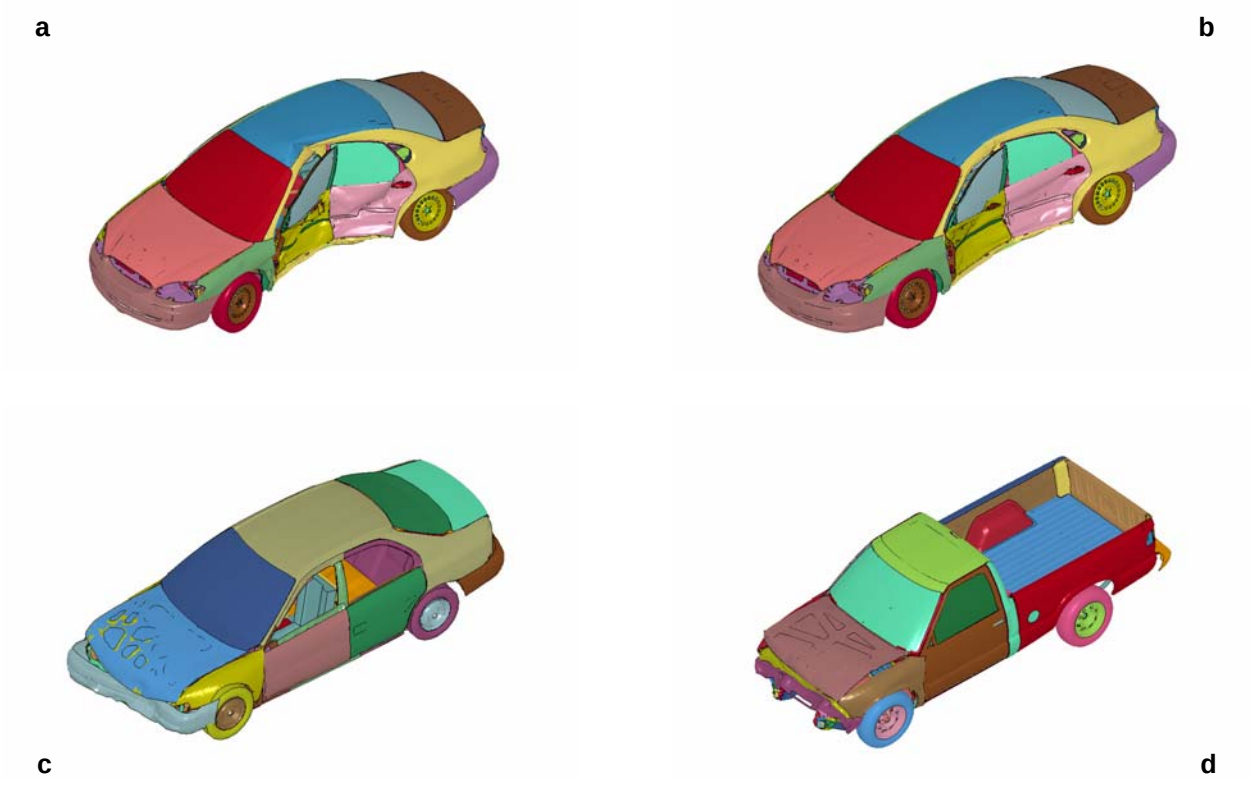


Figure 4: The deformation patterns of the four simulated case vehicles (V1) for case #2000-79-149 (a), case #1997-11-207 (b), case #1997-82-214 (c), and case #1998-72-98 (d).

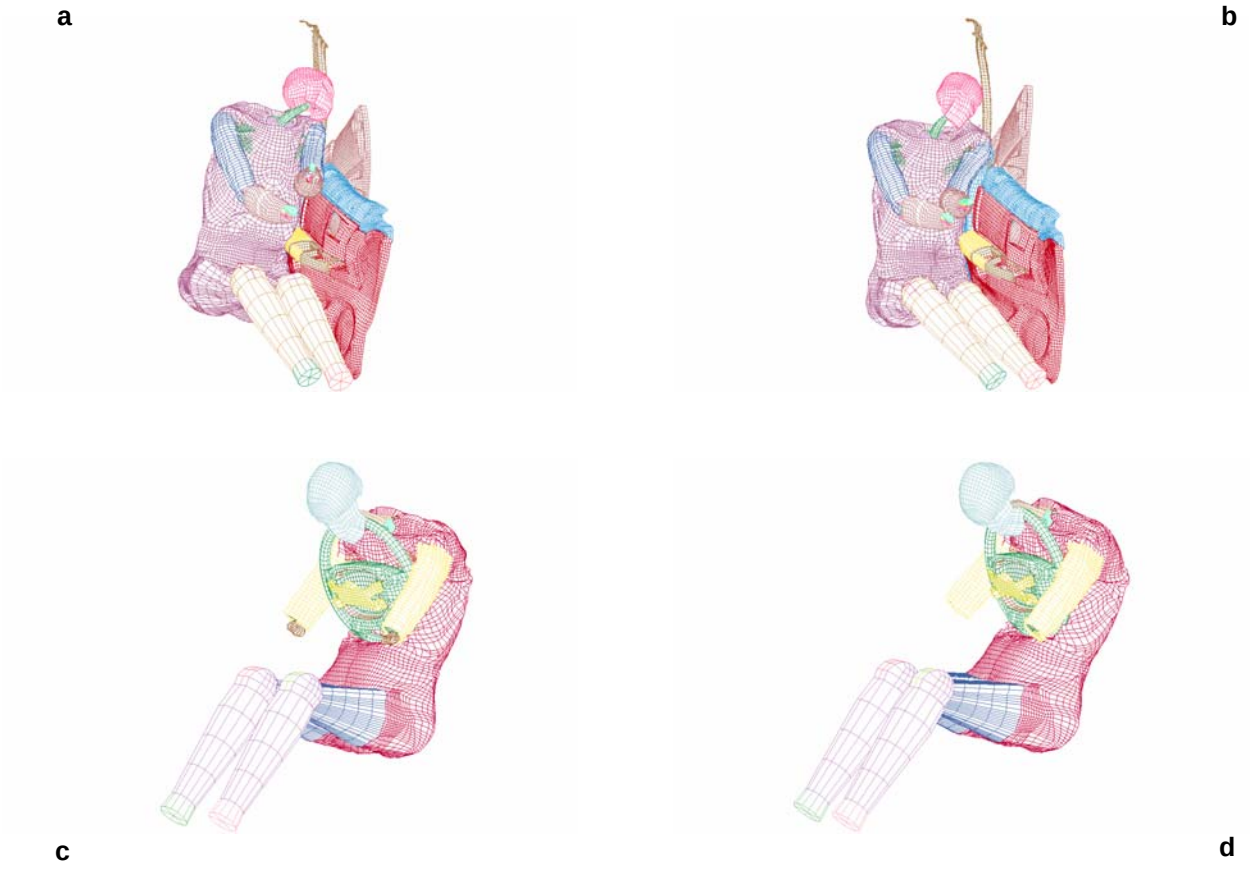


Figure 5: The FE occupant interaction with the sub-modeled vehicle components at the time of maximal contact for case #2000-79-149 (a), case #1997-11-207 (b), case #1997-82-214 (c), and case #1998-72-98 (d).

Table 3. Peak Average Aorta Responses For The FE Simulations.

| Case # | Stress (MPa) | | | Strain | | |
|---|---|---|---|---|---|---|
| | True | | Von-mises | Maximum Principal | Lagrange | |
| | Longitudinal | Circumferential | | | Longitudinal | Circumferential |
| 2000-79-149 | 1.28 | 0.51 | 1.68 | 0.160 | 0.123 | 0.032 |
| 1997-11-207 | 1.03 | 0.48 | 1.60 | 0.153 | 0.125 | 0.035 |
| 1997-82-214 | 0.93 | 0.93 | 0.97 | 0.072 | 0.059 | 0.062 |
| 1998-72-98 | 1.58 | 1.86 | 1.77 | 0.152 | 0.099 | 0.157 |
| Avg. | | | | 0.134 | | |


Figure 6: AP (left column) and lateral (right column) perspectives of the inner surface maximum principal strain patterns for the FE aortas simulations from case #2000-79-149 (a), case #1997-11-207 (b), case #1997-82-214 (c), and case #1998-72-98 (d).

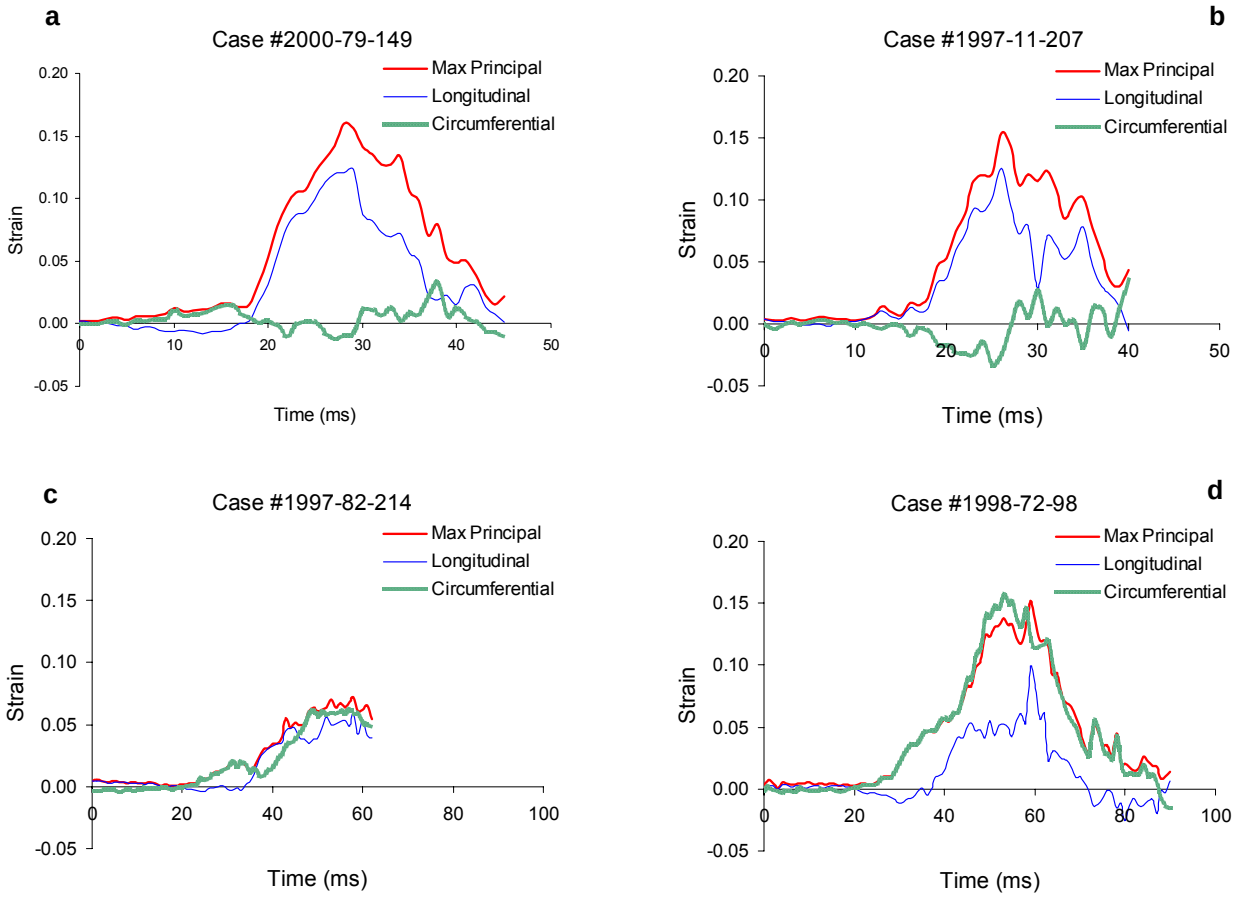


Figure 7: The time histories for the average maximum principal, longitudinal and circumferential Lagrange strain for the FE aortas simulations from case #2000-79-149 (a), case #1997-11-207 (b), case #1997-82-214 (c), and case #1998-72-98 (d).

## DISCUSSION

Four real world crashes with aortic injuries to occupants were simulated using FE techniques. These simulations demonstrate the feasibility of the approach of using FE vehicles and a FE occupant model to investigate the underlying mechanisms of the TRA. No specific autopsy data were available in the NASS data regarding the locations of the aortic injuries for any of the cases. This made direct comparison between the simulation results and the real-world injury data impossible. Shah et al. (2005a) were able to make such direct comparison and found an excellent match between regions of high strain in the model and actual injury data. However, the peri-isthmic region is known to be preferentially injured (Katyal et al., 1997), and to be relatively weak compared to other sections of the aorta (Lundevall, 1964). Therefore, the simulation results are interpreted with respect to the peri-isthmic region, and the average stress and strain values were calculated for this region. The near side-impact cases exhibited highest strain in the peri-isthmic region. The frontal impact cases resulted in highest strain in the arch at the junction with the ascending aorta, followed by the peri-isthmic region. The insertion of the ligamentum arteriosum can create large strains at the point of insertion. However, since tears tend to initiate a distance from the insertion, the stress and strain values immediately at the insertion were not used for analysis. Compressive values were ignored. The relatively high stress and strain demonstrated in the peri-isthmic region of the model suggests the model response could be indicative of the actual injuries sustained in the crashes. Comparison to aorta failure thresholds is needed to provide a more complete understanding of the response and model limitations.

The FE simulations resulted in peak average longitudinal true stress ranging from 0.93 to 1.58 MPa (Table 3), which overlaps the lower end of the failure range shown in Table 4. The FE peak average maximum principal strain ranged from 0.072 to 0.160, which is roughly half the failure level derived from Shah et al. (2005b) on average. The longitudinal and circumferential Lagrange strains are also lower than the derived thresholds. As mentioned, the average longitudinal strains from the near side-impact simulations are considerably greater than the circumferential strains, and follow the time-history trends of the average maximum principal strains. The reverse is true for the frontal impact simulations, but the resulting average strains are still below threshold. These results suggest that the FE simulations predict peri-isthmic injury relative to stress but not strain. However, this depends entirely upon the material law used to represent the aorta tissue, which in this case is linear elastic with Young's modulus based on Shah et al. (2005b). A new material law should be implemented based on new material properties of Shah et al. (2005b; 2006).

Table 4. Aorta Failure Thresholds Derived From Shah et al. (2005b).

| Test | True Stress (MPa) | | Strain | | |
|---|---|---|---|---|---|
| | Longitudinal | Circumferential | Maximum Principal | Lagrange | |
| | | | | Longitudinal | Circumferential |
| A | 1.39 | 1.72 | 0.265 | 0.252 | 0.170 |
| B | 1.59 | 1.89 | 0.346 | 0.258 | 0.289 |
| C | 2.31 | 2.47 | 0.301 | 0.232 | 0.205 |
| D | 1.31 | 1.54 | 0.280 | 0.186 | 0.257 |
| E | 2.05 | 1.60 | 0.414 | 0.334 | 0.347 |
| Avg. | 1.73 | 1.84 | 0.321 | 0.252 | 0.254 |

The FE model demonstrates relative high strain at the junction of the ligamentum arteriosum and aorta for each simulation. This is considered to be a necessary artifact, and is assigned little importance. This is because clinically the ligament is not seen to separate from the aorta, and sections of relative high stress and strain are seen throughout the peri-isthmic region. However, the ligamentum arteriosum representation seems to be related to abrupt shape changes in the arch (similar to a "kinked" garden hose) for some simulations. This kinked shape develops as the ascending aorta joins the arch as well.

There are a number of issues associated with the whole-body human FE model. It is fully validated against a variety of external inputs (Shah et al. 2001; 2004; 2005a). This constitutes a macroscopic level of validation only. The model used in this study benefited from the addition of the pericardium and parietal pleura, which are thought to be important to TRA mechanisms. However, there exists an artificial influence of the superior vasculature due to an abrupt termination and therefore tethering of the vessels at the neck. Further, there is no representation of the musculature beneath the manubrium that attach to the viscera of the aortic arch. Similarly, there is no representation of the ligaments that tether the pericardium to the gladiolus. These structures are likely to be important to the mechanisms of TRA in side impact, in which anterior motion of the sternum due to rib deflection and force along the clavicles tends to pull the heart and arch away from the spine. However, the FE model contains a representation of the pericardium and central tendon, so motion of the heart is influenced by motion of the diaphragm, which may be important to TRA also.

A particular modeling challenge was the first phase of simulation: the car-to-car reconstructions. The exact model vehicles were not always available in the NCAC library. Therefore, the closest approximating vehicles were selected and scaled. The complete effect of this procedure is unknown, but is thought to be small compared to other issues. Since the deformation values match reasonably this is not first order limitation in simulating car-to-car simulation. Another challenge was the front end representations of some of the vehicles. In some cases the structures were too stiff to produce the required crush values. In other cases structures were missing, requiring sections to be added to achieve the proper front end and bumper profiles. In general, attaining crush characteristics close to the measured deformation values was difficult and required multiple first-phase simulations to produce reasonably matching numbers.

Another factor influenced the second phase of simulation: the occupant position and posture. Little data were available in the NASS database to help with locating and orienting the whole-body model within the vehicles. Estimates were obtained from combining accident investigation photographic records with subject anthropometry. The total effect of these estimates on occupant kinematics and interactions with interior vehicle structures is unknown, but is potentially substantial.

A final consideration is the constitutive properties used for the FE representation of the aorta and other mediastinal structures. Sufficient data do not exist to formulate an appropriate representation. Additional efforts such as those of Maddali et al. (2005) and Shah et al. (2005b; 2006) will assist in this endeavor.

## CONCLUSIONS

Traumatic rupture of the aorta has been studied using finite element simulations. A two-stage finite element approach has been implemented for the simulation of reconstructed, real-world, car-to-car collisions. The results of this study provide a better understanding of the possible mechanisms associated with TRA. Finite element simulation demonstrates regions of relative high stress and strain in the peri-isthmic region for near side-impact cases, which is indicative of that seen clinically. Finite element simulation demonstrates regions of relative high stress and strain in the peri-isthmic region and the junction of the ascending aorta and arch for frontal impact cases. Substantially more work is needed to produce a locally validated finite element representation of the human mediastinal contents.

## ACKNOWLEDGMENTS

The funding for this research has been provided [in part] by private parties, who have selected Dr. Kennerly Digges [and FHWA/NHTSA National Crash Analysis Center at The George Washington University] to be an independent solicitor of and funder for research in motor vehicle safety, and to be one of the peer reviewers for the research projects and reports. Neither of the private parties have determined the allocation of funds or had any influence on the content of this report.

This research was supported in part also by the National Highway Traffic Safety Administration through the Southern Consortium for Impact Biomechanics of the University of Alabama at Birmingham.

## REFERENCES

BURKHART, H. M., GOMEZ, G. A., JACOBSON, L. E., PLESS, J. E., and BROADIE, T. A. (2001). Fatal Blunt Aortic Injuries: A Review of 242 Autopsy Cases. J Trauma, 50, 113-115.

CAMMACK, K., RAPPORT, R. L., PAUL, J., and BAIRD, W. C. (1959). Deceleration injuries of the Thoracic Aorta. A.M.A. Archives of Surgery, 79, 244-251.

CRASS, J. R., COHEN, A. M., MOTTA, A. O., TOMASHEFSKI, J. F. JR, and WIESEN, E. J. (1990). A proposed new mechanism of traumatic aortic rupture: the osseous pinch. Radiology, 176(3), 645-649.

DOSIOS, T. J., SALEMIS, N., ANGOURAS, D., and NONAS, E. (2000). Blunt and Penetrating Trauma of the Thoracic Aorta and Aortic Arch Branches: An Autopsy Study. J Trauma, 49, 696-703.

HASS, G. M. (1944). Types of internal injuries of personnel involved in aircraft accidents. Journal of Aviation Medicine, 15, 77-84.

IWAMOTO, M., MIKI, K., MOHAMMAD, M., NAYEF, A., YANG, K. H., BEGEMAN, P. C., and KING, A. I. (2000). Development of a Finite Element Model of the Human Shoulder. 44th Stapp Car Crash Journal, 44, 281-297.

KATYAL, D., MCLELLAN, B. A., BRENNEMAN, F. D., BOULANGER, B., SHARKEY, P. W., and WADDELL, J. P. (1997). Lateral impact motor vehicle collisions: Significant cause of blunt traumatic rupture of the thoracic aorta. Journal of Trauma, 42(5), 769-772.

KLOTZ, O. and SIMPSON, W. (1932). Spontaneous Rupture of the Aorta. American Journal of Medical Science, 184, 455-473.

LEE, J. B. and YANG, K. H. (2001). Development of a finite element model of the human abdomen. 45th Stapp Car Crash Journal, 45, 79-100.

LETTERER, E. (1924). Beitrage zur entstehung der aortenruptur an typischer stele. Virch. Arch. Path. Anat, 253, 534-544.

LUNDEVALL, J. (1964). The Mechanism of Traumatic Rupture of the Aorta. Acta Path. Microbiol. Scand, 62, 34-46.

MADDALI, M., SHAH, C. S., and YANG, K. H. (2005). Finite Element Modeling of Aortic Tissue Using High Speed Experimental Data. Proceedings of IMECE05, 2005 ASME International Mechanical Engineering Congress, IMECE2005-82083.

MATTOX, K. L. (1989). Fact and fiction about management of aortic transaction. Ann Thorac Surg, 48, 1--2.

McGWIN, G., METZGER, J., MORAN, S. G., and RUE, L. W. (2003). Occupant- and Collision-Related Risk Factors for Blunt Thoracic Aorta Injury. J. Trauma, 54, 655-662.

NEWMAN, R. J., and RASTOGI, S. (1984). Rupture of the thoracic aorta and its relationship to road traffic accident characteristics. Injury, 15, 296-299.

OPPENHEIM, F. (1918). Gibt es eine spontanrupter der gesunden aorta und wie kommt sie zustande. Münchener Medizinische Wochenschrift, 65, 1234-1237.

SAUAIA, A., MOORE, F. A., MOORE, E. E., et al. (1995). Epidemiology of trauma deaths: a reassessment. J. Trauma, 38, 185-193.

SHAH, C. S., HARDY, W. N., MASON, M. J., YANG, K. H., VAN EE, C. A., MORGAN, R., and DIGGES, K. (2006). Dynamic Biaxial Tissue Properties of the Human Cadaver Aorta. 50th Stapp Car Crash Journal, 50, 217-246.

SHAH, C. S., LEE, J. B., HARDY, W. N., and YANG, K. H. (2004). A Partially Validated Finite Element Whole-Body Human Model for Organ Level Injury Prediction. Proceedings of IMECE04, 2004 ASME International Mechanical Engineering Congress, IMECE2004-61844.

SHAH, C. S., MADDALI, M., MUNGIKAR, S. A., BEILLAS, P., HARDY, W. N., YANG, K. H., BEDEWI, P. G., DIGGES, K., and AUGENSTEIN, J. (2005a). Analysis of a Real-World Crash Using Finite Element Modeling to Examine Traumatic Rupture of the Aorta. Occupant Safety, Safety-Critical Systems, and Crashworthiness, SAE Paper No. 2005-01-1293.

SHAH, C. S., MASON, M. J., YANG, K. H., HARDY, W. N., VAN EE, C. A., MORGAN, R., and DIGGES, K. (2005b). High-Speed Biaxial Tissue Properties of The Human Cadaver Aorta. Proceedings of IMECE05, 2005 ASME International Mechanical Engineering Congress, IMECE2005-82085.

SHAH, C. S., YANG, K. H., HARDY, W. N., WANG, K. H., and KING, A. I. (2001). Development of a computer model to predict aortic rupture due to impact loading. 45th Stapp Car Crash Journal, 45, 161-182.

STEPS, J. (2003). Crash Characteristics Indicative of Aortic Injury in Near Side Vehicle-to-Vehicle Crashes. Ph.D. Dissertation, The George Washington University.

STRASSMANN, G. (1947). Traumatic Rupture of the Aorta. American Heart Journal, 33, 508-515.

VOIGT, G. E. and WILFERT, K. (1969). Mechanisms of injuries to unrestrained drivers in head-on collisions. Proc. 13th Stapp Car Crash Conference, pp. 295-313.

ZEHNDER, M. A. (1960). Accident Mechanism and Accident Mechanics of the Aortic Rupture in the closed Thorax Trauma. Thoraxchirurgie und Vasculaere Chirurgie, 8, 47-65.

# DISCUSSION

PAPER: **Investigation of traumatic rupture of the aorta (TRA) using simulated real-world accidents involving aortic injuries**

PRESENTER: ***C.S. Shah, Bioengineering Center, Wayne State University***

**Q**UESTION: *Joel Stitzel, Wake Forest University*
I promise I'm not up here just in defense or to bring an attack. I actually did have a question. We do, in fact, have a fencing team at Virginia Tech. We have a former student, actually in the lab, who was a fencer. Anyway, I had a question about what's filling an aorta? How do you model the aorta in terms of what's inside of it during these events?

**A**NSWER: We use the linear fluid ABAC model -- so it's basically incompressible fluid inside there, inside the aorta.

**Q:** So what's the density of the linear fluid? You're using, like, an air approach where--?

**A:** It's more closer to the water, I would say.

**Q:** The density's closer to water?

**A:** Yes.

**Q:** In the linear fluid approach, is the density taken into account in the effect of that mass on the pressures, on the inner wall? My impression on the linear fluid airbag was that it was a constant volume air where the pressure changes throughout the exact moment of defamation of that volume. It doesn't really take into account pressure waves that might move through the tissue or, kind of, local events, you know, of movement of—

**A:** Well, even though, for our aorta model, we held a closed boundary at the termination of the aorta. So even though it's a closed volume approach, you know, any impact, solid impact will produce a pressure wave because of the volume change. But, we didn't try to simulate the exact blood flow or the pressure pulse for the blood. That we didn't try.

**Q:** Right. Thanks.

**Q:** *Guy Nusholtz, Daimler Chrysler*
It's not clear what you're trying to accomplish. You're sort of mimicking four crashes, but you don't really have the initial condition and you don't really have the right cars. So, what are you trying to do: just say that you could possibly get high strains in the aorta under these conditions? And the reason for this is: Why would you bother even trying to mimic crashes? Why don't you just take your human body model and load in a couple of different loading conditions, which could occur in a crash, and then see the different type of spans of injuries, or pressures that you would see – pressures and strains? Why would you want to reproduce for crashes when you're not even getting close to what the initial conditions are?

**A:** I think we did the same thing in 2001 when I presented the staff model: used the thorax model to impact from seven different directions and we tried to see the strain and stress in the aorta. For this particular thing, even though it's not mimicking exactly the same initial condition in terms of the occupant or in terms of the vehicles, we are trying to see whether these kind of crashes, which involve aortic injury: What is the outcome of the model? Whether the model is mimicking the same scenario or whether it's way off of the—And, we are also hoping that we will do some parametric analysis by changing the initial conditions, as well as different vehicles and different energy levels. So that will help us in evaluating what exactly is happening to the aorta with that situation.

**Q:** But you don't have anything to compare it to. I mean, you don't have the outcome. You don't have the initial conditions.

**A:** Well, we—

**Q:** It just seems very confusing.

**A:** Well, we do have the threshold for all the regions so far and we conducted the tension test for the aorta. And, we do have the filial threshold in terms of strain for the aorta.

**Q:** But, none of that adds into why you're trying to reproduce crashes. All of it—That would all relate to a parametric study. Say, okay, here's the threshold. If I load it like this or if I change the loading conditions slightly, then these are the types of things I'd expect to see. It's just not clear why you'd want to try and sort of pseudo-produce crashes, which are not really, which really didn't occur. Anyways, it's just a very confusing—

**A:** Maybe Warren can help me a little bit with that.

**Q:** Okay.

**Q:** *Warren Hardy, Bioengineering Center - Wayne State University*
Yeah, well this is actually still very much a work-in-progress, and we have a long way to go before we can truly address some of the issues that you've raised. One thing: Other than taking the model and exercising it in a parametric that Chirag has already done—In fact, we can do further with a car-to-car scenario, we are interested in seeing what types of interaction, occupant interactions with the vehicle might get us in a situation where we might suspect traumatic rupture of the aorta. We do have more data coming down the pipeline here where we have much more detailed autopsy information, perhaps a little more information about the original occupant position, etc., etc. That, of course, is a real black box in this whole thing and we may never get to the point where everybody's satisfied with what we're doing. But, there are also other folks that are interested in looking at other aspects of the vehicle response and perhaps coming up with predicted algorithms for TRA from that end. Personally, that's not our specific interest, but there are folks that are interested in doing that. More or less taking what we know, building upon other aspects of our TRA investigations and trying to apply that in an actual—well, in a simulated automotive environment and seeing what different occupant interactions with vehicle structures might have something to do with TRA. That's kind of where we're headed, but we still have a long way to go. So, that's some of the thinking behind it. I don't know if that helps.

**Q:** *Steve Rouhana, Ford Motor Company*
Chirag, nice work. Although I am an Adjunct at Wayne State, I won't get into the saber rattling of—I'll get right to the point. [laughter] I couldn't help noticing during your playing of the FE models of the whole body that there seemed to be a bit of extension in the head-neck region. In the frontal impact, the head seemed to go over the steering wheel and in the side impact, there was a lot of sheer and what looked like making the neck longer. And it seemed to me that that might add to your likelihood of having this traumatic rupture of the aorta because of the connection of the carotid artery on the left side and the brachial cephalic trunk on the right side. Did you explore that at all?

**A:** Well, one of the things that we had aberrant connection of those arteries at the neck, so we really are not simulating the tension in carotid and, you know—That might be a point and yeah, it could affect the stretching in the arch or ascending region. And most likely, we'll be heading to modeling of the neck. Also, we are probably going to include those arteries along with the neck. That may be a more realistic approach. Yeah.

**Q:** I may say that the boundary condition there is important.

**A:** Yes. That's correct.

**Q:** Okay. Thanks.